Adv. Space Res. Vol. 9, No. 1, pp. (1)233–(1)243, 1989
Printed in Great Britain.

0273–1177/89 $0.00 + .0

SNOW DIELECTRIC MEASUREMENTS

A. Denoth

Institute of Experimental Physics, University of Innsbruck, A–6020 Innsbruck, Austria

ABSTRACT

Measurements of the dielectric constant and of the dielectric loss of Alpine snow with various stages of metamorphism are reported. The measurements covering the frequency range of up to 1GHz have been carried out in the natural snow cover; measurements in the microwave X-band (8 to 12 GHz) were recently made with natural snow samples in the laboratory. The effects of snow porosity, grain size and shape and snow wetness are studied in detail and are compared to model calculations. On the basis of experimental results battery-powered dielectric devices for snow wetness measurements in the field have been developed. As water content and water distribution in the uppermost snow layers are important quantities in remote sensing studies in the decimeter and centimeter wavelength regime, the geometry of the sensors has been designed to allow nearly non-destructive surface and volume measurements of the water content. Measurements of a vertical dielectric profile and of daily variations in the wetness gradient in the natural snow cover are shown.

INTRODUCTION

Electromagnetically, snow is a heterogeneous three-component dielectric material consisting of ice particles or ice clusters, air and liquid water. The dielectric function of both ice and water depend on frequency and temperature /1,2,3/. For that reason, the dielectric function of snow also depends on frequency and temperature and is controlled by the volume fractions, type of distribution and shapes of the individual components. In general, effects of particle size may be neglected in the low- and radio-frequency range /4/. At frequencies exceeding a few GHz, however, effects of particle size on the attenuation of wet snow samples have been observed experimentally /5/. For the measurement of the dielectric function of snow over a wide frequency range various measuring techniques are used: In the LF and RF regime ac-bridges and resonance methods have prooved their efficiency /6/; in the VHF and microwave regimes free-space transmissions techniques /5,7-10/ and closed or open resonator techniques are applied /11-13/. For the modeling of the electromagnetic behaviour of snow, however, wideband dielectric data are needed; as snow, especially if wet, is thermodynamically a rather instable system, the measurements of the dielectric properties should be made as quick as possible.

In this study wideband dielectric data of snow with various stages of metamorphism are reported. Data measurements were performed within a few minutes using two automatic network analyzer systems. As an engineering application of the experimental results a dielectric measuring device has been developed that can be used to determine snow liquid water content in the field /14/. As liquid water content and wetness gradients in near-surface layers are very usefull ground-truth parameters for the interpretation of remote sensing observations, the geometry of the flat-plate sensors has been designed to allow rapid and nearly non-destructive measurements. To achieve a sufficient spatial resolution, the effective measurement depth of the sensors should be in the range of 1 to 3 cm. The effective measurement depth can be adjusted by varying the width and spacing of the coplanar electrodes /6,15/. Measurements of daily variations of snow surface wetness and wetness gradients with these sensors are included in this study.

MEASUREMENT TECHNIQUES

Different sensors have been used to measure the dielectric function of snow in the frequency range from 100 Hz up to 10 GHz. In the lower frequency range from 100 Hz up to 50 MHz a simple plate condenser consisting of 5 stainless-steel plates of 10 x 13 cm^2 effective area, a spacing of 27 mm of the electrodes and with 20 pF effective measuring capacitance in air is used as sensor. The frequency dependence of the sensor impedance in snow is automatically recorded by a low-frequency network analyzer (type R&S ZPV with tuner unit E1). A block dia-

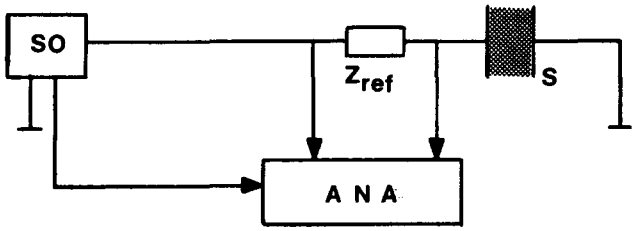

Fig. 1. Block diagramm of the low-frequency measuring system. SO: sweeper-oscillator, ANA: network analyzer, S: snow sample, impedance Z, Z_{ref}: reference impedance.

gramm of the low-frequency measuring system is shown in Figure 1. To achieve high accuracy in the impedance measurements, the value of the reference impedance Z_{ref} varies with frequency, so that the ratio Z/Z_{ref} does not deviate much from unity. A measurement with this system over the frequency range of 100 Hz to 50 MHz with 9 data points per frequency decade takes approximately 1 minute.

In the higher frequency range of 50 MHz to 1 GHz the real part of the dielectric function, ε' has been derived from the shift in the resonance frequency of short thin monopole antennas as nearly non-destructive sensors /14,16/. The shift in frequency was measured through recording the variation with frequency of the input reflection coefficient using the same network analyzer type R&S ZPV with tuning unit E3. To allow measurements of a wide range of permittivities ε' three monopole antennas with different lengths of 6 cm, 9.1 cm and 17.2 cm with resonant frequencies in air of 1230 MHz, 810 MHz and 420 MHz, respectively, can be mounted in the center of a large aluminium disk. In addition, to increase the accuracy in the measurements of the dielectric function of the relatively low-loss material snow (in the 100 MHz to 1 GHz frequency range), test measurements of the input impedance of a monopole probe have been performed using a HP8510A network analyzer system. The antenna input impedance is controlled by the geometrical dimensions of the monopole, the frequency, and the propagation constant of the medium /17/. The dielectric function can be derived from the input impedance by an iterative process.

In the microwave X-band, the dielectric function of snow has been derived by measuring the complex transmission and reflection coefficient of a large snow sample located between two horn antennas. The antennas are mounted vertically in order to minimize effects of possible horizontal snow inhomogeneities. A block diagramm of the X-band free-space transmission system is shown in Figure 2. The measurements in the X-band have been made in a cold-room in the laboratory, using a HP 8510A network analyzer system.

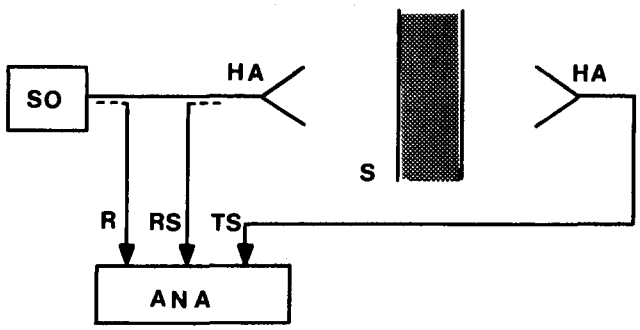

Fig. 2. Block diagramm of the X-band measuring system. SO: sweeper-oscillator, HA: horn antenna, S: snow sample, ANA: automatic network analyzer, R: reference signal, RS: reflected signal, TS: transmitted signal.

In order to account for the influence of different texture properties on the dielectric function, the snow samples have been classified according to their mean grain size and shape, and porosity ϕ. Grain shape is related to the mean axial ratio of the grains; it can be derived from an analysis of snow photographs /4/, whereby the ice grains are assumed to be oblate

spheroids. Snow porosity, ϕ, is calculated from snow density, ρ, the density of ice, ρ_i ($\rho_i \simeq 0.917$ g/cm^3), and the liquid water content, W, according to:

$$\phi = 1 - (\rho - \rho_w.W)/\rho_i \quad (1)$$

ρ_w is the density of water at 0°C. Snow liquid water content W has been measured by a freezing calorimeter. The field measurements have been carried out in the Stubai Alps, Austria.

EXPERIMENTAL SNOW DIELECTRIC DATA

The typical dielectric response of Alpine snow in the frequency range of 100 Hz up to 10 GHz is demonstrated with a dry and a wet snow sample in the Figures 3a and 3b and in Figure 4. The quasi-continuous measurements of the dielectric function in the lower frequency range of 100 Hz to 50 MHz are represented in the figures by a solid line (data points are not shown). In the higher frequency range of 50 MHz to 10 GHz, the measured data points are shown and are connected through a dotted line.

In Figure 3 the dielectric function of a dry sample of new snow, shape factor of the oblate ice grains $g_i \leq 0.04$, porosity $\phi = 0.64$, and snow temperature T = -3°C, is plotted against frequency (in Hz) on a logarithmic scale. Figure 3a shows permittivity ε', and Figure 3b shows the losses and the power attenuation α (dB/km). In the microwave regime the losses are very low, $\varepsilon'' \leq 10^{-3}$, and therefore subject to large errors when measured by a free-space transmission technique. In Figure 4 the dielectric function of a wet sample of old snow, grain shape factor $g_i \simeq 0.23$, porosity $\phi = 0.43$, water content W = 1.08% by volume, snow temperature T = 0°C and mean grain size d ~ 1.5 mm is shown against frequency (in Hz) on a logarithmic scale. In the lower frequency regime, f ≤ 50 MHz, the power attenuation α (dB/km) is also shown.

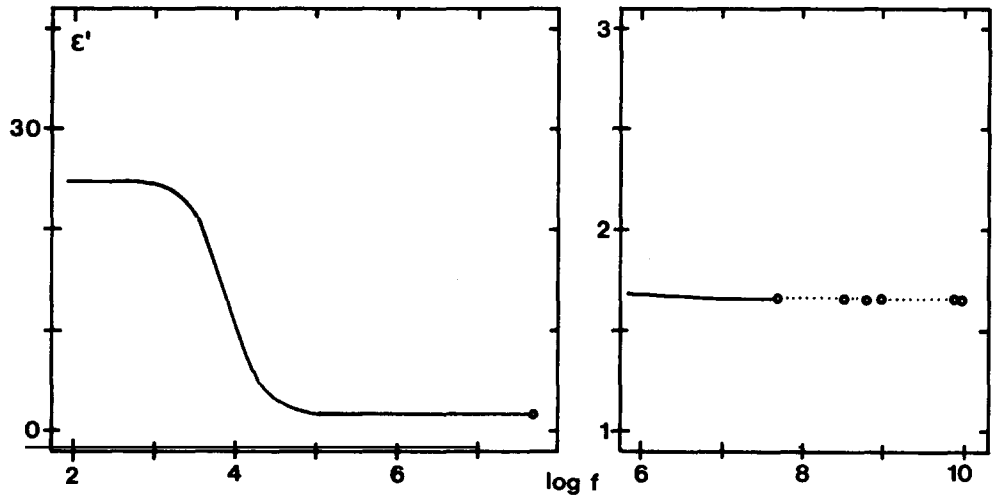

Fig. 3a. Frequency dependence (f in Hz) of permittivity ε' of a dry new snow

The permittivity ε' of both dry and wet snow decreases monotonically with increasing frequency. The relatively high value of ε' in the VLF-regime (f ≤1kHz) is due to the large static dielectric constant of the components ice and - if present - water and to additional polarization effects in granular materials (interfacial polarization). At frequencies higher than a few MHz, snow permittivity ε' becomes independent on frequency and remains constant to approximately 10 GHz (dry snow) or 2 GHz (wet snow); ε' of wet snow decreases slightly for frequencies higher than approximately 2 GHz due to relaxation processes in the water component in this frequency range /1/.

The losses ε'' in snow are determined by the dielectric losses and by losses caused by the ionic conductivity. The sharp increase in the losses of both dry and wet snow samples at VLF-frequencies is due to the ionic component. The peak in the loss in the range of 10 kHz is caused by the dielectric absorption of the ice component /18/. With increasing frequency, the losses decrease monotonically in the case of dry snow samples; the power attenuation is nearly constant in the HF-regime, and is approximately $\alpha \simeq 2$ dB/100m. The losses for wet snow samples, however, pass through a minimum in the 50 to 500 MHz range and show an increase in the GHz range due to the dielectric absorption of water in the microwave X-band. Power attenuation increases drastically from α ~ 0.1dB/m at ~500 MHz to α ~ 50dB/m in the X-band.

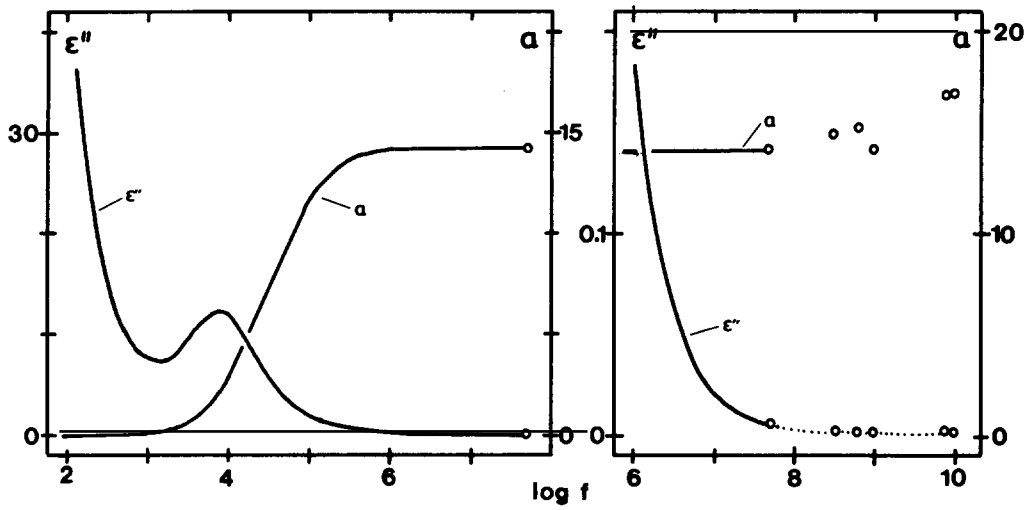

Fig. 3b. Frequency dependence (f in Hz) of the losses ε'' and the power attenuation α (dB/km) of a dry snow sample.

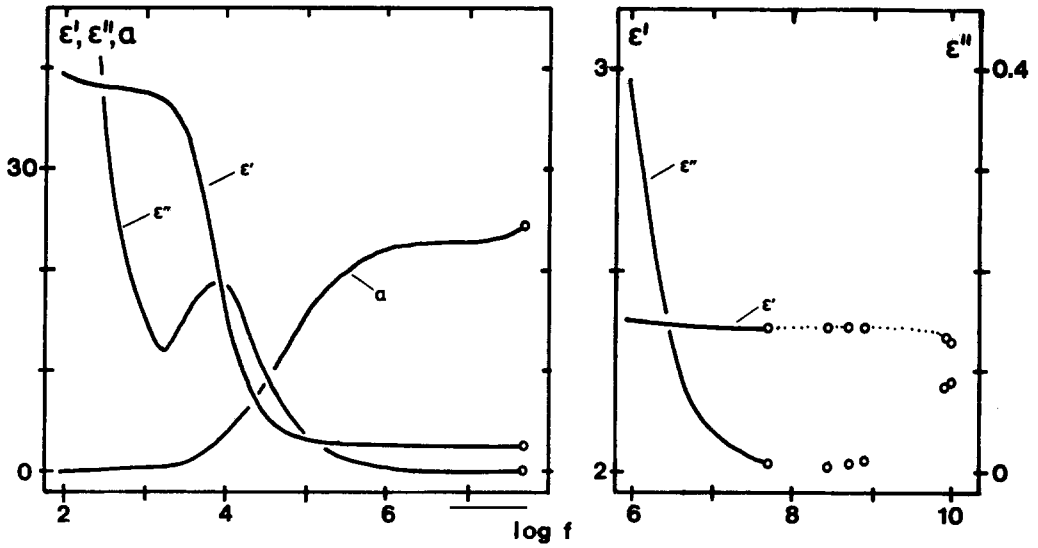

Fig. 4. Frequency dependence (f in Hz) of the dielectric function and power attenuation α (dB/km) of a wet sample of old snow.

EXPERIMENTAL RESULTS AND THEORETICAL MODELS

The three-component dielectric mixture theory of Polder and van Santen /19/ has been shown to satisfactorily describe the dielectric function of snow over a wide range of frequencies /13, 20,21/. This theory allows to account for the distribution and shape of both the ice grains and the liquid water component. Originally, the geometry of the components was assumed to be of ellipsoidal shape; non-symmetrical or irregular shaped components, however, can be built-up by a weighted sum of ellipsoidal sub-components /22,23/. The three-component mixture theory has been used to model the measured dielectric function of snow with various stages of metamorphism and various liquid water contents, whereby the shape factors g_w for the (oblate) water component were taken from Denoth /24/. To a first approximation, the ice grains and the liquid inclusions were assumed to be of spheroidal shape. Experimental results and model calculations are shown in the following figures, Figure 5 to Figure 9.

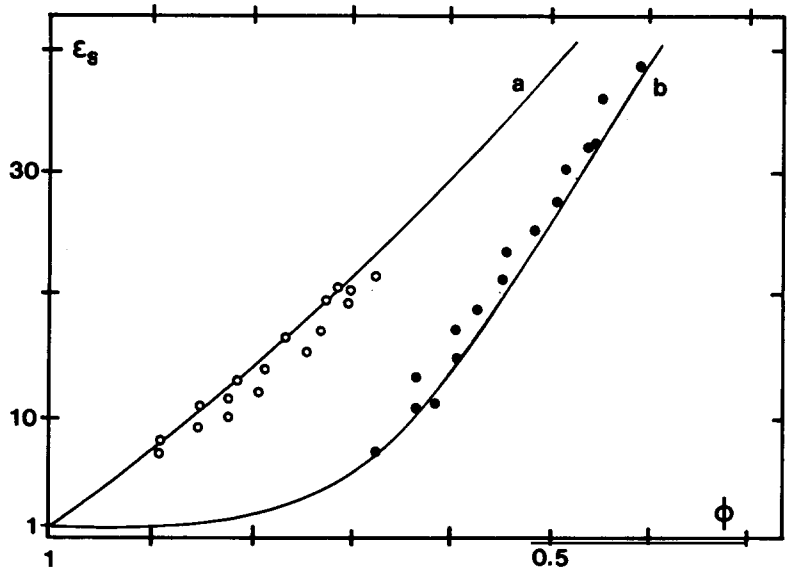

Fig. 5. Static permittivity ε_s as a function of dry snow porosity ϕ. New snow is shown by open circles, and firn samples are represented by closed circles.

Figure 5 shows the static permittivity ε_s as a function of porosity for dry snow samples with limiting stages of metamorphism: new snow (represented by open circles) and multi-year firn with well rounded mm-sized ice grains (represented by closed circles). The solid lines represent model calculations for the static permittivity with different shape factors of the ice component, corresponding to the boarderline cases of snow metamorphism: $g_i = 0.00$ (a) represents new snow with disc-shaped snow flakes, and $g_i = 1/3$ (b) represents ice spheres. From the fact that the static permittivity is independent on the shape of the liquid inclusions but, in contrast, is significantely influenced by the shape of the ice particles results that VLF measurements offer a possibility to determine grain shape factors.

10-MHz-data of the dielectric function of dry snow samples are given in the Figures 6a and 6b as a function of porosity; the solid lines represent model calculations. Snow temperature varied between -5°C and 0°C. The losses, Figure 6b, are shown for limiting cases of snow metamorphism: new snow (open circles) and multi-year firn or old summer snow with well rounded grains (closed circles). Only a small influence of snow wetness on ε'' has been observed: ε'' at 10 MHz is mainly determined by snow texture and the effects of ionic conductivity. For snow porosities $\phi \geq 0.3$ the ε'-data can well be represented by:

$$\varepsilon'_d = 1 + 1.76(1 - \phi) + 0.37(1 - \phi)^2 \qquad (2)$$

which, for practical applications, is more convenient than calculations according to the Polder-van-Santen model.
10-MHz-data of the incremental permittivity $\Delta\varepsilon'$ for wet snow samples are shown in Figure 7 together with model calculations. $\Delta\varepsilon'$ is defined as:

$$\Delta\varepsilon' = \varepsilon'(\text{wet}) - 1 - 1.76(1 - \phi) - 0.37(1 - \phi)^2 \qquad (3)$$

For practical applications, the ε'(wet)-data can well be represented by:

$$\varepsilon' = 1 + 1.92\rho + 0.44\rho^2 + 0.187W + 0.0045W^2 \qquad (4a)$$

or

$$\Delta\varepsilon' = 0.206W + 0.0046W^2 \qquad (4b)$$

whereby W is the volumetric water content in %, ρ is the density of wet snow; cross-terms in $\rho.W$ in equation (4a) are neglected. As ε' is independent on frequency from 10 MHz up to approximately 2 GHz, equations (4a) and (4b) are also valid in this frequency range.

X-band-data for $\Delta\varepsilon'$ and α are shown in the Figures 8a and 8b for a selected frequency of 10 GHz. The solid lines represent model calculations for different shapes g_w of the water component (oblate water inclusions): $g_w = 0.008$ and $g_w = 0.08$, respectively. $\Delta\varepsilon'$ and particularly α are controlled by snow wetness and the shape of the water component. The influence of the shape of the ice grains, however, can be neglected. The relatively large scatter in the α - data is due to the fact, that the actual distribution function of the water shape-factors is not known; it is replaced in the model calculations by a mean shape factor, which, in ge-

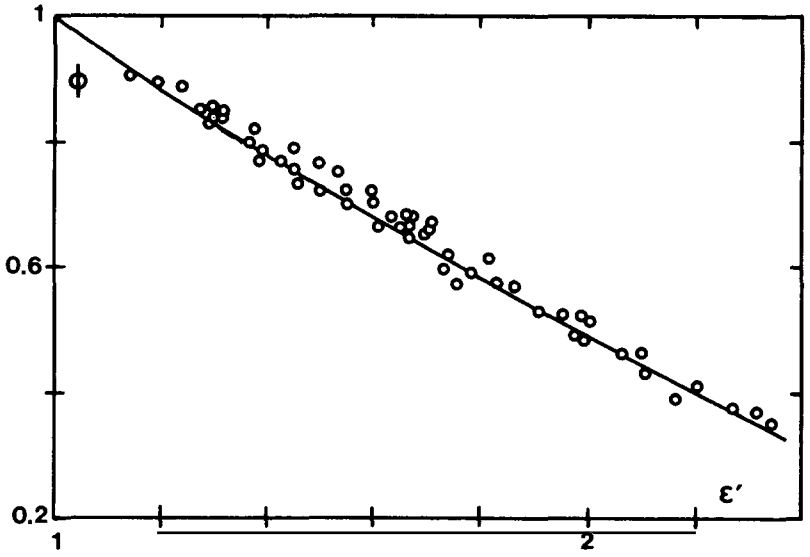

Fig. 6a. Dependence of dry snow permittivity on porosity. Frequency: 10 MHz.

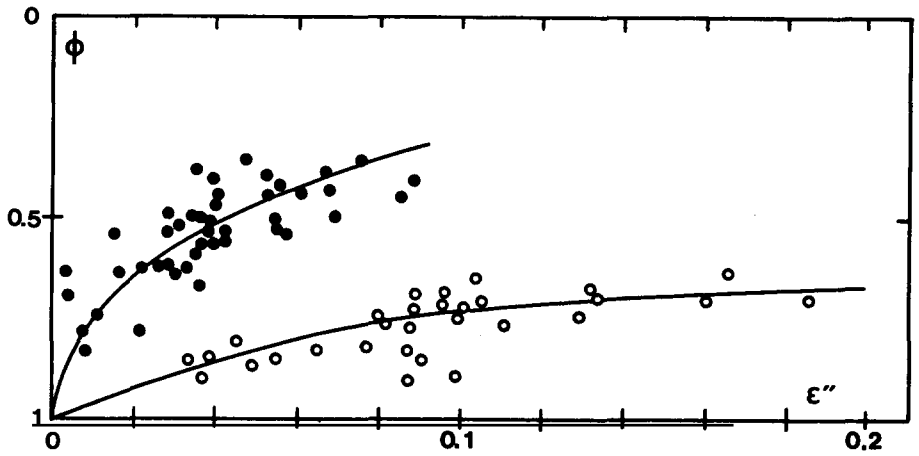

Fig. 6b. Dependence of the losses ε″(10MHz) on snow porosity. New snow is shown by open circles; old snow samples are shown by closed circles.

neral, leads to a underestimation of α. So, better results may be obtained by assuming a non-symmetrical shape of the water component and by replacing the mean value by a weighted sum over a spectrum of shape factors.

A compilation of the relative significance of the parameters W, g_i, g_w and ϕ for the dielectric function at three frequency ranges, VLF (f ≪1 kHz), RF (~10MHz) and X-band, selected with respect to practical applications, is given in Table 1. The calculations have been made for two values of the water content W, W = 0% and W = 5%, a mean porosity ϕ = 0.5 and assuming an oblate spheroidal shape of the ice and water components. Its results: from the static permittivity grain shape factors g_i can be deduced. In the RF-regime, the water content W, g_w and ϕ determine ε′; grain shape, however, shows no significant influence. The losses ε″ in the RF-regime are determined by W and ϕ; nevertheless, ε″ cannot be used for the determination of snow wetness W, as in this relatively low frequency range the effects of ionic conductivity cannot be neglected. Furthermore, the losses are relatively low, ε″ ≲ 0.2, and low losses are not easy to measure in the field with the required accuracy. In X-band, both ε′ and ε″ are determined by W, g_w and ϕ in nearly the same way as in the RF-regime. The dielectric loss ε″, however, is mostly controlled by W and the shape of the water inclusions. With respect to the dominant effect of W and g_w, the influence of snow porosity on ε″ can be neglected.

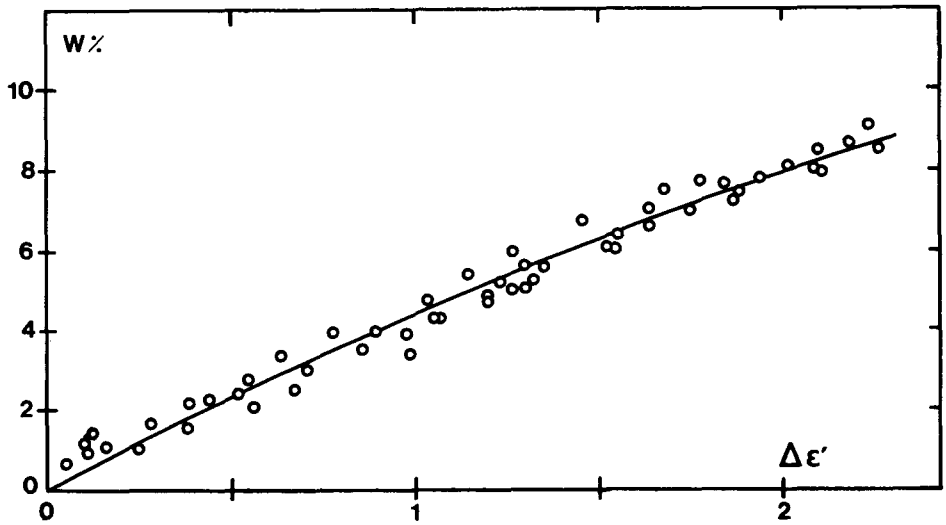

Fig. 7. Dependence of the incremental permittivity $\Delta\varepsilon'$(10MHz) on snow wetness W (% by volume). The solid line represents a calculation according to equation (4b).

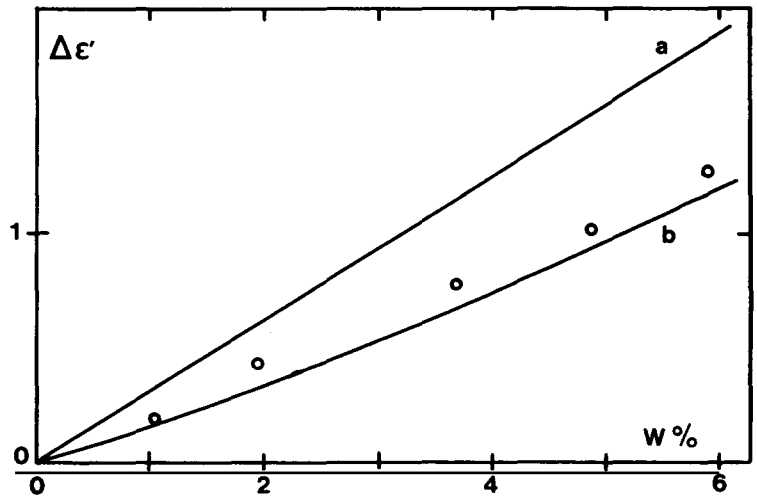

Fig. 8a. Dependence of the incremental permittivity $\Delta\varepsilon'$(10GHz) on snow wetness W (% by volume). The solid lines are model calculations for g_w = 0.008 (a) and g_w = 0.08 (b).

INTERCOMPARISON OF DIELECTRIC DATA

Relations between ε' and density ρ of dry snow, especially suited for practical applications, are given in Table 2. The frequency range of measurements and the range of validity with respect to snow density, and references are also given. Although the relations look very different, the results are very similar. Table 3 shows a compilation of empirical relations between $\Delta\varepsilon'$ or ε'' respectively, and water content W. The frequency range of measurements and references are also given.

Calculations according to the different empirical relations unfortunately result in more or less different values for the dielectric function. One reason may be that the dielectric function at these frequencies is highly influenced by the shape of the water component, and the liquid shape is controlled by both the water content itself and the stage of metamorphism of the snow sample. So, a general valid simple relation between $\Delta\varepsilon'$ or ε'' and liquid water content W may not exist.

DIELECTRIC SNOW WETNESS METERS

As a technical and practical application of snow dielectric measurements in the RF-regime, snow wetness meters for both surface and volume wetness measurements have recently been developed. Snow wetness is calculated from the measured snow permittivity ε' at 20 MHz and snow density according to equation (4a). Snow density has to be measured separately. Flate-plate

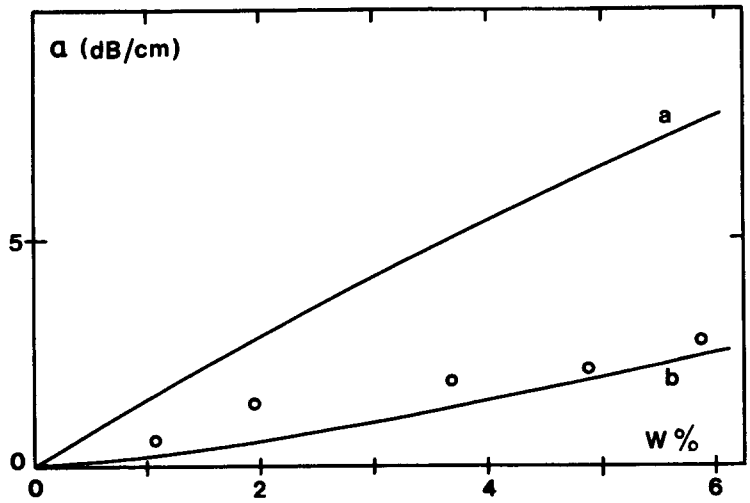

Fig. 8b. Dependence of the power attenuation coefficient α (10GHz) in dB/cm on snow wetness W (% by vol.). The solid lines represent model calculations for $g_w = 0.008$ (a) and $g_w = 0.08$ (b).

TABLE 1 Relative Significance of ϕ, W, g_i and g_w for the Dielectric Function (ε', ε'') at three Frequencies.

	VLF (f ≤ 1kHz)		RF (f 10MHz)		X - band	
	W = 0%	W = 5%	W = 0%	W = 5%	W = 0%	W = 5%
$(\delta\varepsilon'/\delta\phi)/\varepsilon'$	-3.5	-2.9	-1.2	-1.0	-1.2	-1.0
$(\delta\varepsilon'/\delta W)/\varepsilon'$	3.5	2.8	34	13	24	10
$(\delta\varepsilon'/\delta g_i)/\varepsilon'$	-1.5	-1.0	-0.1	0	-0.1	0
$(\delta\varepsilon'/\delta g_w)/\varepsilon'$	--	-0.1	--	-7.5	--	-4.0
$(\delta\varepsilon''/\delta\phi)/\varepsilon''$	—	—	-3.0	-2.0	-3.0	-1.1
$(\delta\varepsilon''/\delta W)/\varepsilon''$	—	—	7.0	6.0	100	35
$(\delta\varepsilon''/\delta g_i)/\varepsilon''$	—	—	-0.3	0	0.4	0
$(\delta\varepsilon''/\delta g_w)/\varepsilon''$	—	—	--	0.2	—	-20

TABLE 2 Empirical Relations between ε' and Density ρ of Dry Snow

Empirical Relation	Remarks		References
$\varepsilon' = (1 + 0.851\rho)^2$		f ≥ 10 MHz	/25/
$\varepsilon' = (1 + 0.508\rho)^3$		f = 9.375 GHz	/21, 26/
$\varepsilon' = 1 + 1.582 / (1 - 0.365\rho)$ *	$\rho \leq 0.45$	f = 1 GHz	/27/
$\varepsilon' = 1 + 2.22\rho + 0.41\rho^2$		f = 3.48 MHz	/28/
$\varepsilon' = 1 + 2.0\rho$		4 ≤ f ≤ 12 GHz	/5/
$\varepsilon' = 1 + 1.9\rho$	$\rho \leq 0.5$	3 ≤ f ≤ 18 GHz	/9, 21/
$= 0.51 + 2.88\rho$	$\rho \geq 0.5$		
$\varepsilon' = 1 + 1.92\rho + 0.44\rho^2$	$\rho \leq 0.65$	0.01 ≤ f ≤ 1 GHz	/29/
$\varepsilon' = 1 + 1.70\rho + 0.70\rho^2$		f = 1 GHz	/11/

* The original empirical relation given in reference /27/ has been improved with new measurements.

sensors with differently sized and shaped coplanar conducting stripes are used for a nearly non-destructive measurement of ε'. The width and spacing of the electrodes has been optimized to achieve both a sufficient spatial resolution of approximately ±1.5 cm and to average over a sufficiently large number of snow grains /6,14/. A photograph of one of these sensors, connected to the control and display unit, is shown in Figure 9. The snow wetness meters are battery-powered and can be operated at ambient temperatures down to -10°C.

TABLE 3 Empirical Relations between $\Delta\varepsilon'$ or ε'' and Snow Wetness

Empirical Relation	Remarks	References
$\Delta\varepsilon' = 0.206W + 0.0046W^2$	$0.01 \leq f \leq 1$ GHz	/13/
$\Delta\varepsilon' = 0.02W + (0.06 - 3.1\ 10^{-4}(f-4)^2)W^{1.5}$	$4 \leq f \leq 12$ GHz	/5/
$\Delta\varepsilon' = a.W + b(f).W^{1.5}$	$f \geq$ GHz	/10/
$\Delta\varepsilon' = 0.089W + 0.0072W^2$	$f = 1$ GHz	/11/
$\varepsilon'' = 0.073\ \sqrt{\varepsilon'}\ W / f$	$4 \leq f \leq 12$ GHz	/5/
$\varepsilon'' = 0.009W + 0.0007W^2$	$f = 1$ GHz	/11/
$\varepsilon'' = c(f)\ W^{1.5}$	$f \geq$ GHz	/10/

A measurement of the dielectric and wetness profile of a natural snow cover with these sensors is shown in Figure 10. The measurement procedure, including density measurements, with a total of 31 data points, was performed within 15 minutes. The relatively sharp peaks in the water content at a height of 180 cm and 200 cm above ground are caused by two thin snow/ice layers with a drastically reduced hydraulic conductivity. Wetness gradients and time-variations in the gradients can also be detected with a fine spatial resolution. As an example, the dielectric profile within a 12 cm thick surface snow layer, measured under clear-sky conditions in march 1987 at an altitude of 950m is shown in Figure 11; the measurements have been made at 10:00, 12:00, 15:30 and 18:00, respectively. The surface gradient $d\varepsilon'/dz$ is slightly negative in the morning, $d\varepsilon'/dz = -0.03\ cm^{-1}$, and increases to $d\varepsilon'/dz = -0.33\ cm^{-1}$ at 12:00. At 15:30, the gradient changes its direction and becomes positive, $d\varepsilon'/dz = 0.04\ cm^{-1}$, and increases to $d\varepsilon'/dz = 0.34\ cm^{-1}$ in the late afternoon. From the displacement of the peaks of ε' with time a velocity of $v \approx 1.5$ cm/h can be deduced; this velocity can be interpreted as the speed of a penetrating meltwater wave.

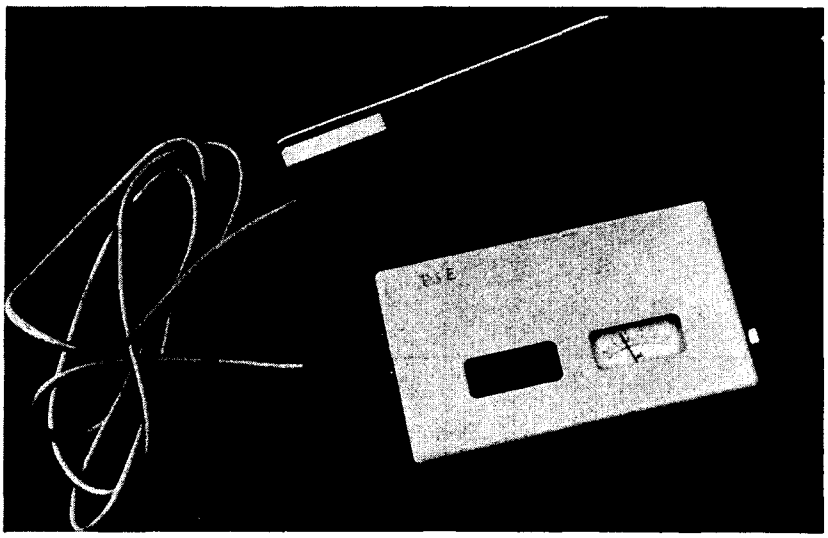

Fig. 9. Photograph of the snow wetness meter. A flate-plate sensor is connected to the tuning and display unit.

CONCLUSION

From this study of wide-band frequency behaviour of the dielectric function of snow the following conclusions can be made: The 3-phase Polder-van-Santen model is applicable to describe the dielectric behaviour of snow, whereby the ice component can be assumed to be of oblate spheroidal shape; a non-symmetrical shape, however, may be preferred for modeling the dielectric function in the GHz-regime. The static dielectric function can be used to deduce shape factors for the ice grains, if porosity and water content are measured separately; it reflects therefore snow texture properties.
The real part of the dielectric function in the RF-regime can be used for snow wetness determinations if separate density measurements are made. The total losses of snow are determined in this frequency regime by both the dielectric losses and the ionic losses. In the microwave regime, snow permittivity depends on porosity and water content; the dielectric losses, however, are very sensitive to the water content and the shape of the water inclusions. An influence of the grain size on the dielectric function has not been observed in the whole

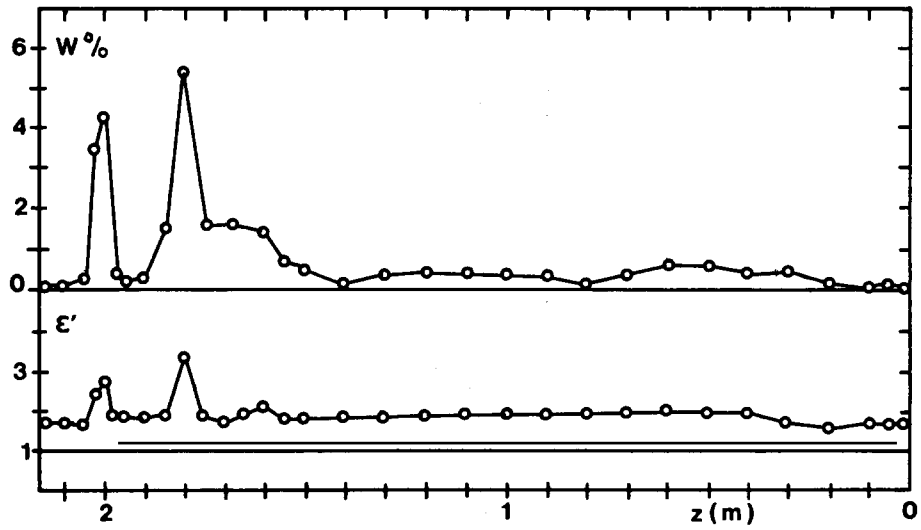

Fig. 10. High-resolution dielectric and wetness profile of a natural snow cover. z is given in meters above ground.

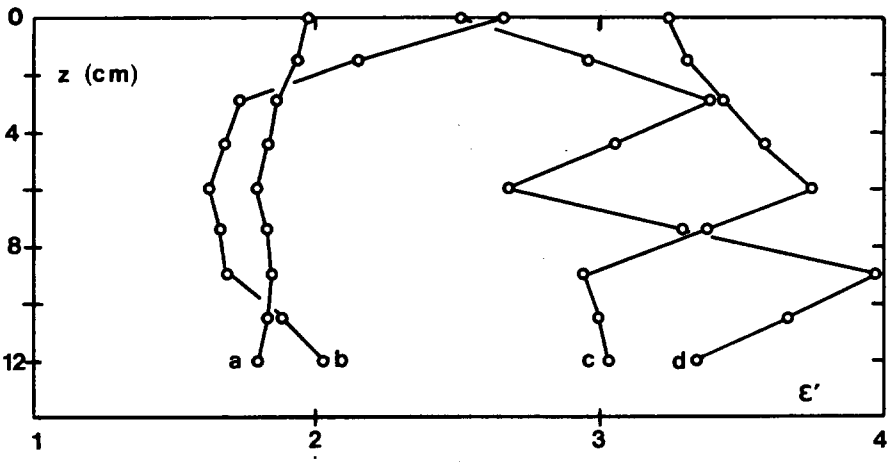

Fig. 11. Daily variation of a dielectric profile in a 12 cm surface snow layer. Measurements are made at 10:00 (a), 12:00 (b), 15:30 (c) and 18:00 (d).

frequency range of up to 10 GHz.
So, for dielectric modeling, additional precise measurements of the dielectric function are needed in the microwave regime, to increase the data base for deducing appropriate liquid shape factors and their variation with snow metamorphism.

ACKNOWLEDGEMENT

This study was supported in part by the Austrian "Fonds zur Förderung der wissenschaftichen Forschung", Grant numbers: P4525 and P5907. The "Wintersport Tirol AG" is thanked for supporting the field activities in the Stubai Alps.

REFERENCES

1. J.B. Hasted, Aqueous Dielectrics, Chapman and Hall, London, 1973
2. S. Evans, Dielectric properties of ice and snow - A review. J. Glac. 5, 773 (1965)
3. C. Mätzler, and U. Wegmüller, Dielectric properties of fresh-water ice at microwave frequencies, Z. Physik D: Appl. Phys., 20, 1623 (1987)
4. A. Denoth, Effect of grain geometry on electrical properties of snow at frequencies up to 100 MHz, J. Appl. Phys., 53, 7496 (1982)
5. W.I. Linlor, Permittivity and attenuation of wet snow between 4 and 12 GHz, J.Appl.Phys. 51, 2811 (1980)

6. W. Ambach, and A. Denoth, The dielectric behaviour of snow, a study versus liquid water content, NASA CP 2153, ed. A. Rango, Goddard Space Flight Center, 1980, p. 69
7. J. Tobarias, P. Saguet, and J. Chilo, Determination of the water content of snow from the study of electromagnetic wave propagation in the snow cover, J. Glac., 20, 585 (1978)
8. K. Yamamoto, S. Kusu, and K. Higuchi, Dielectric properties of wet snow in the microwave region, Report Water Resources Inst., Nagoya University, Japan, 1984
9. M. Hallikainen, F.T. Ulaby, and N. Abdelrazik, The dielectric behaviour of snow in the 3- to 37 GHz range, Proc. IGARSS'84, Strasbourg 1984, p 169
10. J. Chilo, V. Liva, and A. Coumes, Proprietés physiques de la neige et propagation en ondes centimetriques, in: Elektronik und Lawinen '79. ed. Inst.f. Elektronik d. TU Graz, Graz 1983, p. 44
11. M. Tiuri, A. Sihvola, E. Nyfors, and M. Hallikainen, The complex dielectric constant of snow at microwave frequencies, IEEE J. Oceanic Eng., OE-9,5, 377 (1984)
12. C. Mätzler, H. Aebischer, and E. Schanda, Microwave dielectric properties of surface snow IEEE J. Oceanic Eng., OE-9,5, 366 (1984)
13. A. Denoth, A. Foglar, P. Weiland, C. Mätzler, H. Aebischer, M. Tiuri, and A. Sihvola, A comparative study of instruments for measuring the liquid water content of snow, J. Appl. Phys., 56, 2154 (1984)
14. A. Denoth, and A. Foglar, Recent developments of snow moisture dielectric devices, in: ISSW 86, Homewood, CA 96718, 1986, p. 72
15. A. Foglar, Entwicklung eines Schneefeuchte-Meßgerätes zur Wassergehaltsbestimmung in dünnen Schichten, Diploma thesis, University of Innsbruck, 1983
16. H. Aebischer, Methoden zur Messung der Schneefeuchte mit Hilfe von Mikrowellen, Diploma thesis, University of Berne, 1983
17. S.C. Olson, and M.F. Iskander, A new in situ procedure for measuring the dielectric properties of low permittivity materials, IEEE Transact. Instr. and Meas., IM-35, 2 (1986)
18. P.V. Hobbs, Ice Physics, Clarendon Press, Oxford, 1974
19. D. Polder, and J.H.van Santen, The effective permeability of mixtures of solids, Physica 12, 257 (1946)
20. S.C. Colbeck, The geometry and permittivity of snow at high frequencies, J.Appl.Phys., 53, 4495 (1982)
21. F.T. Ulaby, R.K. Moore, and A.K. Fung, Microwave remote sensing, Artech House, Dedham, MA 0206, 1986
22. H. Chaloupka, Gewinnung einiger geometrischer Strukturdaten aus der Frequenzabhängigkeit des elektromagnetischen Streuverhaltens, Kleinheubacher Berichte, 23, 51 (1980)
23. H. Chaloupka, O. Ostwald, and B. Schieck, Structure independent microwave moisture measurements, J. Microwave Power, 15, 221 (1980)
24. A. Denoth, The pendular-funicular liquid transition and snow metamorphism, J.Glac.,28, 357 (1982)
25. G. Robin, Radio echo sounding: Glaciological interpretation and applications, J.Glac., 15 49 (1975)
26. W.A. Cumming, The dielectric properties of ice and snow at 3.2 cm, J. Appl. Phys., 23, 768 (1952)
27. C. Mätzler, Applications of the interaction of microwaves with the natural snow cover, Remote Sensing Reviews 2, 259-387 (1987)
28. Z. Yosida, H. Oura, D. Kuroiwa, T. Huzioka, K. Kojima, and S. Kinosita, Physical studies on deposited snow, Report 14, Low Temp. Sci. Inst., Hokkaido University, Sapporo, Japan, 1958
29. A. Denoth, and A. Foglar, Measurement of daily variations in the subsurface wetness gradient, Annals of Glac., 6, 254 (1985)